J Mater Sci (2007) 42:2766–2774
DOI 10.1007/s10853-006-1420-x

Fracture behaviours of epoxy nanocomposites with nano-silica at low and elevated temperatures

Shiqiang Deng · Lin Ye · Klaus Friedrich

Received: 4 January 2006 / Accepted: 14 February 2006 / Published online: 12 January 2007

Abstract An investigation was conducted to characterize fracture behaviours of nano-silica modified epoxies at low and elevated temperatures. A nano-silica dispersed epoxy (Nanopox XP 22/0516, Hanse-Chemie, Germany) with 40 wt% silica nano-particles was used as modifier to toughen an epoxy resin, Araldite F (Bisphenol A based, Ciba-Geigy). Fracture toughness and other mechanical properties were measured using standard compact tension (CT), tensile and flexural specimens to elaborate the effects of nano-silica particles on fracture behaviours of epoxy nanocomposites at different temperatures, –50, 0, 23, 50 and 70 °C. Dynamic mechanical analysis (DMA) was utilized to define the glass transition temperature (T_g) upon the addition of different amounts of nano-silica particles. Fracture toughness of the nano-silica modified epoxies was clearly increased at 23 °C and 50 °C, but the role of nano-silica particles in enhancing the fracture toughness became less pronounced at 0 °C and –50 °C and disappeared at 70 °C.

S. Deng · L. Ye (✉)
Centre for Advanced Materials Technology, School of Aerospace, Mechanical and Mechatronic Engineering, The University of Sydney, Sydney, NSW 2006, Australia
e-mail: ye@aeromech.usyd.edu.au

K. Friedrich
Institute for Composite Materials, University of Kaiserslautern, 67663 Kaiserslautern, Germany

Introduction

As widely used thermosetting polymers, epoxy resins have several unique characteristics, high adhesive strength, high strength and hardness, excellent chemical and heat resistance. Epoxies have been widely used in various industrial applications, particularly as adhesives for bonding and as matrix resins for producing high-performance fibre reinforced composites. However, most cured epoxy systems show low fracture toughness, poor resistance to crack initiation and propagation, and inferior impact strength. For example, delamination and poor impact resistance of fibre reinforced epoxy composites is often attributed to the low fracture toughness of epoxy matrix. Many efforts have been made in the past decades to improve the fracture toughness of epoxies by modifying epoxy resins with additives such as rubbers, thermoplastics, and inorganic particles. However, though effective, the addition of some modifiers, for example rubbers and thermoplastics, can result in reductions of basic mechanical properties, such as decreases in strength, modulus and glass transition temperature, T_g [1]. Research work conducted by Bascom et al. [2] revealed that fracture energy (G_{IC}) was increased significantly up to approximately 30 times that of the unmodified epoxy with an increase in the volume fraction of rubber content from 4.5 to 20%, while the tensile strength, tensile modulus and T_g decreased drastically in a roughly linear rate with the amount of rubber added to the epoxy system. Many thermoplastic polymers have also been used as additives with epoxies to the aim of improving fracture toughness [3], but not all attempts were successful because of poor compatibility between a

thermoplastic modifier and the epoxy resin as well as poor processability in the use of thermoplastic modifiers. However, inorganic additives, such as silica, alumina and glass particles, have been found in recent years to be more promising modifiers for increasing the fracture toughness of epoxies without sacrificing their basic properties [4, 5]. More recently there has emerged a new technology based on the formation of a nano-phase structure, consisting of small rigid particles or fibres with a diameter (or at least one dimension) of less than 100 nm dispersed in epoxy matrixes, which holds a great promise for increasing the mechanical performance of epoxies without compromising other desirable mechanical and thermal properties of the modified systems.

When nano-particles are used as modifiers in epoxies, a homogeneous dispersion is required in order to achieve the nano-phase structure. As the particles tend to agglomerate, special techniques have had to be developed and used to achieve a homogeneous particle distribution, including mechanical mixing using high shear forces and ultrasonic vibration. Chemical methods have also been used such as a sol-gel process to obtain nano-silica particles, in which the nano-particles are commonly formed in situ during a sol–gel manufacturing process and thus a homogenous dispersion is readily achieved [6, 7]. It has been demonstrated that the addition of low concentrations of nano-silica particles (about 1–8% by mass) to a typical rubber-toughened epoxy adhesive leads to very significant increases in both the toughness of the adhesive and T_g as well as the single-lap shear strength at the ambient temperature [6]. Some recent studies also showed that nano-sized silica particles produced by the sol–gel process can noticeably improve fracture toughness and other mechanical properties of epoxies at ambient temperature [8] and at cryogenic conditions [9]. As epoxies are normally used in a variety of environmental conditions which cover a wide range of temperatures from subzero to elevated temperatures, it is essential to elaborate the effectiveness of inorganic nano-particles in toughening epoxies throughout a wide range of environmental temperatures.

In this work, an attempt is made to characterize the fracture behaviour of a nano-silica modified epoxy system under a wide range of temperatures from –50 °C to 70 °C. Fracture toughness and other material properties are measured using standard specimens in order to identify the effects of the nano-additives on the fracture behaviours of modified epoxies and to gain a basic understanding of the possible toughening mechanisms.

Experimental

A SiO_2 nano-particle dispersed epoxy (Nanopox XP 22/0516, Hanse-Chemie AG, Germany) was used as a modifier to toughen a diglycidyl ether of bisphenol A (DGEBA) epoxy resin, Araldite-F (Ciba-Geigy, Australia). Nanopox 22/0516 consists of surface-modified silica nano-particles (40 wt%) with an average particle size of 20 nm. As the SiO_2 particles are formed in situ during a sol–gel process, they have a narrow range of particle-size distribution and excellent dispersion in the host epoxy [6]. Despite the relatively high SiO_2 content, the nano-filled epoxy (Nanopox XP) has a comparatively low viscosity and can be easily mixed with epoxies to be modified due to the agglomerate free colloidal dispersion of the SiO_2 nano-particles.

Different amounts of Nanopox XP were mixed with the Araldite F epoxy by means of a mechanical mixer stirring for 30 min at 60 °C to obtain a homogenous mixture. The weight percentage of the nano-silica was selected ranging from 0% to 8%. The mixture was then degassed in a vacuum oven (about –100 kPa) at 100 °C for about 2 h. Upon completion of degassing, the vacuum was released and Piperidine hardener (Sigma Aldrich) was added at a ratio of 100:5 by weight while stirring slowly. The liquid mixture was then cast into preheated moulds and cured at 120 °C for 16 h. The cured epoxy plates were left in the oven and allowed to cool gradually to ambient temperature before removal from the moulds.

Transmission electron microscopy (TEM) was applied to identify the homogeneity of nano-silica particles in the cured epoxies. Figure 1 shows TEM micrographs of the Araldite F epoxies modified with 4 and 8 wt% nano-silica, respectively. The dispersion of the nano-particles in both epoxies is very uniform.

The cured epoxy plates were machined into different specimens for various mechanical tests including compact tension (CT), tension, flexure and dynamic mechanical analysis (DMA), which were conducted at several temperatures, –50, 0, 23, 50 and 70 °C.

Fracture toughness of the cured epoxies was measured using the compact tension (CT) method according to the ASTM standard, ASTM D5045. The CT specimen had a nominal dimension of $48 \times 48 \times 10$ mm, as shown in Fig. 2. A sharp pre-crack was introduced to each CT specimen by a razor blade tapping method to minimize the effects of residual stress and plastic deformation around crack tip [10]. Some as-cured CT specimens were tested at ambient temperature, while the rest of the CT specimens were post-cured at 120 °C for 1 h before testing to minimize residual stress which could be caused by contraction associated with molecular rearrangement during cross-linking in the moulds [11] or induced by the

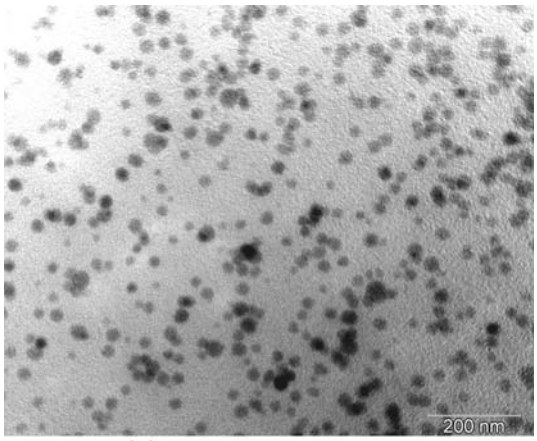

(a) 4 wt% silica modified epoxy

(b) 8 wt% silica modified epoxy

Fig. 1 TEM micrographs of 4 wt% and 8 wt% nano-silica modified epoxies

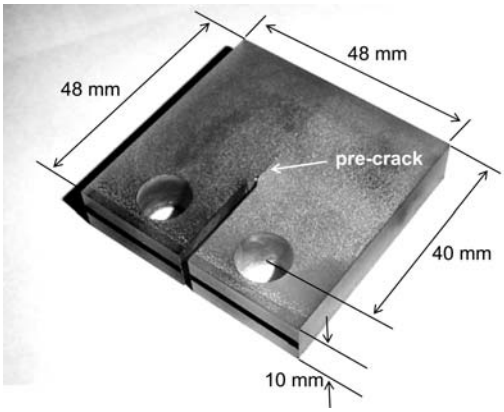

Fig. 2 Compact tension (CT) specimen for fracture toughness measurements

machining process of the CT specimens. A loading rate of 10 mm/min was adopted as recommended by ASTM D5045-99. At least three CT specimens were successfully tested for each group at different temperatures.

Tension and flexure tests were also conducted to measure the basic material properties. The tensile specimen has a dog-boned shape as required by ASTM D 638-99, with a cross section of 10×6 mm at the gauge length region. An extensometer with a gauge length of 50 mm was attached on the tensile specimen surface for determining axial strain. A loading rate of 5 mm/min was selected for all tensile tests. The flexure test specimens had a nominal dimension of $80 \times 12 \times 4$ mm. A supporting span of 50 mm and a loading rate of 2 mm/min were used for all the flexural tests. At least five specimens were tested in both tests for each group at different temperatures. All tensile and flexural specimens were tested at as-cured condition without post-curing.

A universal material testing machine (Instron 5567) was used for all mechanical characterizations including tension, flexure and fracture toughness tests. All tests at low and elevated temperatures were carried out in an environmental chamber. The test chamber allowed reasonably accurate control of the test temperature, which was monitored by two *T* type thermocouples; one thermocouple was placed on the specimen surface, while the other was hanging in the chamber. For the low temperature testing, liquid nitrogen was used to create a low temperature environment by a temperature controller which regulated the liquid nitrogen flow blowing into the chamber according to the temperature required. Once a specimen was mounted and the chamber door was closed, at least 20 min soaking time was maintained to allow the temperature in the chamber to become homogeneous, i.e. the readings from the two thermocouples were the same. For the tests at elevated temperatures, after a specimen was placed in the chamber it was gradually heated up to the designated temperature and then held at that temperature for at least 20 min before the testing began, in order to ensure the uniform temperature distribution within the specimen.

The glass transition temperature (T_g) of the cured epoxies was determined by a dynamic mechanical analyser (TA DMA 2980) with temperature scanning from ambient temperature to 150 °C at a heating rate of 2 °C/min. A single cantilever beam loading fixture was used for the DMA measurements using specimens with dimensions of $30 \times 12 \times 4$ mm. Fracture surfaces of the tested specimens were examined using optical microscopy and scanning electron microscopy (SEM) to identify possible failure mechanisms.

Results and Discussions

Ambient temperature

Figure 3 shows a set of typical load—crack opening displacement (COD) curves obtained from CT tests at

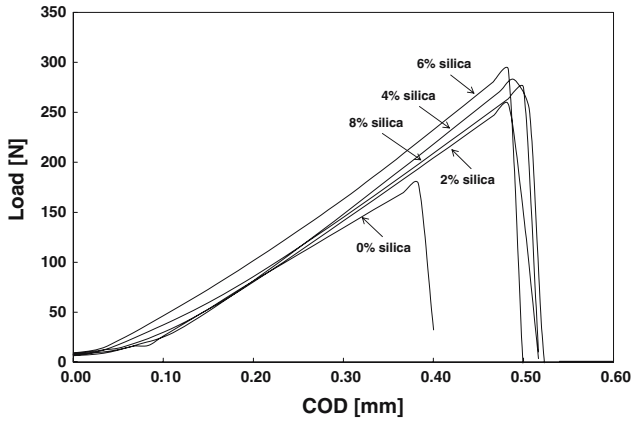

Fig. 3 Typical load—crack opening displacement (COD) curves at RT

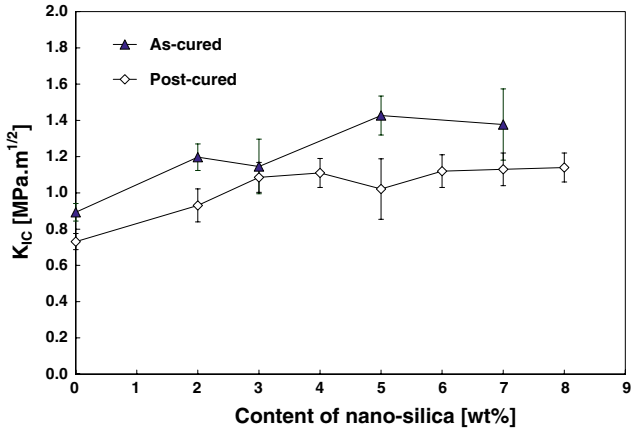

Fig. 4 Fracture toughness (K_{IC}) measured at RT

ambient temperature (RT), 23 ± 2°C, for post-cured epoxy nanocomposites with different amount of nano-silica particles. It can be seen that both pure and modified epoxies undergo unstable crack propagation when the maximum load is reached, while the maximum loads for modified epoxies are obviously higher than for the unmodified counterpart. The values of fracture toughness (K_{IC}) obtained at ambient temperature are shown in Fig. 4 for both the as-cured and the post-cured specimens. Tensile and flexure properties of the as-cured epoxies are shown in Table 1. K_{IC} of the modified epoxies measured by compact tension (CT) in both the as-cured and post-cured conditions was significantly improved after only a small amount of nano-silica was added (2%–8% in weight). For the as-cured epoxies fracture toughness was increased up to 60% from 0.89 MPa $m^{1/2}$ (pure) to 1.43 MPa $m^{1/2}$ (5 wt% silica modified), while for the post-cured epoxies there were also apparent increases in K_{IC} values with increases of nano-silica content, up to 50% from 0.76 MPa $m^{1/2}$ (pure) to 1.14 MPa $m^{1/2}$ (8 wt% silica modified). After post-curing there were slight decreases in K_{IC} for the pure and unmodified epoxies, which can be attributed to an increase in the degree of cross-linking [12]. As evident from the tension and flexure results shown in Table 1, the addition of nano-silica resulted in noticeable increases in the tensile and flexural moduli, and also in a slight increase in tensile and flexural strength.

For rigid inorganic particle-filled epoxies certain toughening mechanisms have been recommended including: (a) an increase in fracture surface area due to crack deflection and crack twisting around particles [13]; (b) enhanced plastic deformation of the epoxy around the particles [14]; and (c) crack front pinning by rigid particles [15]. With a particle size of 20 nm and inter-particle distance of a similar scale (about 20 nm for 4 wt% nano-silica modified epoxy) for the present system, the traditional argument that stress concentration around the particle promotes localised yielding such as shear bands between particles is doubtful. Crack deflection and crack pinning may be important toughening mechanisms in this case, although it is premature to draw conclusions in that regard.

SEM micrographs of fracture surfaces of CT specimens tested at RT are shown in Fig. 4. In the pure epoxy the fracture surface is smooth, implying a brittle cleavage failure, but in the 4 and 8 wt% nano-silica modified epoxies there are somewhat roughened fracture surfaces near the crack tip indicating the occurrence of localized plastic deformation, which could be attributed to the crack deflection and crack pinning effects of the nano-silica particles (Fig. 5).

Table 1 Mechanical properties of nano-silica modified epoxies at room temperature

Nano-silica (wt%)	Tension		Three-point flexure	
	Modulus [GPa]	Strength [MPa]	Modulus [GPa]	Strength [MPa]
0	2.80 ± 0.03	74.9 ± 0.6	2.70 ± 0.14	112.3 ± 2.6
2	2.89 ± 0.07	74.6 ± 0.4	2.84 ± 0.19	118.6 ± 2.5
4	2.98 ± 0.15	75.1 ± 1.2	2.91 ± 0.09	117.8 ± 1.2
6	2.94 ± 0.07	75.3 ± 0.3	3.03 ± 0.12	124.2 ± 2.6
8	3.18 ± 0.12	76.4 ± 0.4	3.19 ± 0.06	124.7 ± 0.7

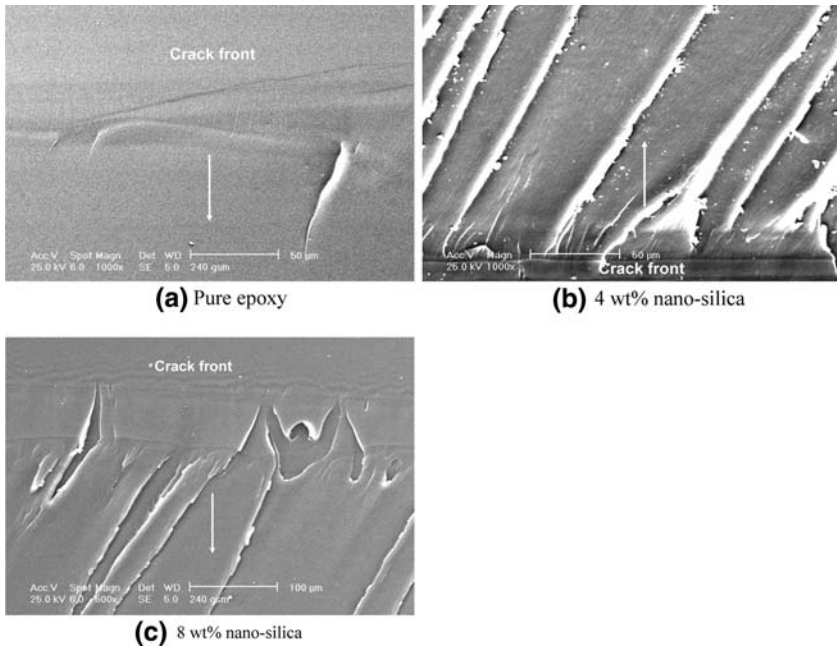

Fig. 5 SEM micrographs of fracture surfaces near crack tips at RT, (**a**) pure epoxy, (**b**) 4 wt% nano-silica and (**c**) 8 wt% nano-silica

Elevated temperatures

The typical load—COD curves obtained from CT tests at 50 °C for epoxy nanocomposites modified with different amount of nano-silica particles are shown in Fig. 6. Similar unstable crack propagation as at RT was observed, while at 70 °C the crack propagation became stable, accompanied by extensive plastic deformation in both unmodified and modified epoxies. The values of K_{IC} at two elevated temperatures, 50 and 70 °C, in comparison with those at RT are shown in Fig. 7. Tensile and flexure properties of the cured epoxies measured at 50 and 70 °C are shown in Table 2. The fracture toughness measured at 50 °C was increased by about 80% from 1.23 MPa $m^{1/2}$ (pure epoxy) to 2.07 MPa $m^{1/2}$ (4 wt% silica modified epoxy), while the strength and modulus of the modified epoxies remain unchanged or was slightly higher with addition of nano-silica. However, there was a slight decrease in K_{IC} at 70 °C with an increase in the content of nano-silica, although K_{IC} for both pure and modified epoxies is increased above 4.0 MPa $m^{1/2}$ (satisfying the condition of plane-strain fracture toughness, ASTM D5045), probably due to the change of failure mechanism from brittle fracture to plastic deformation, as the epoxies become plasticised when the temperature approaches T_g, which is around 100–102 °C. This postulation can be supported by the fracture behaviour of CT specimens shown in Fig. 6, where stable crack propagation with extensive plastic deformation is observed.

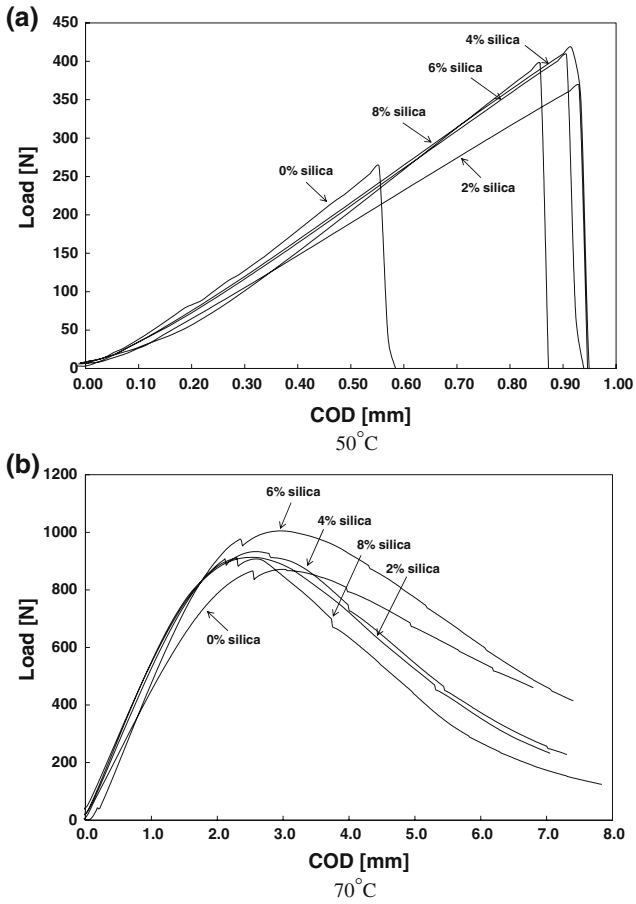

Fig. 6 Typical load—COD curves at 50 °C and 70 °C

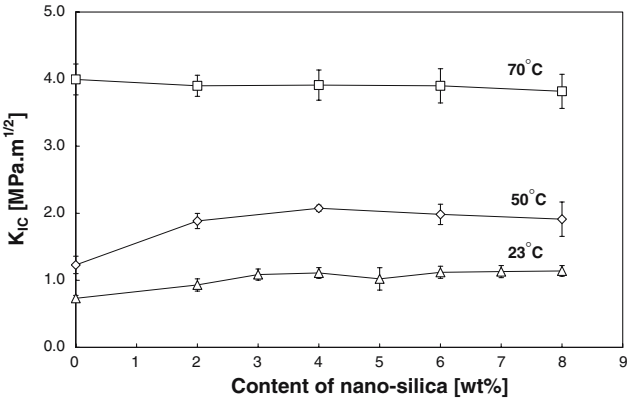

Fig. 7 Fracture toughness of pure/modified epoxies measured at RT, 50 °C and 70 °C

SEM micrographs of fracture surfaces near the crack tip of CT specimens (pure and modified epoxies) tested at 50 °C are shown in Fig. 8. In the pure epoxy specimen, the flat fracture surface indicates a brittle cleavage failure, but for the nano-silica modified epoxy there are clear signs of plastic deformation left on the crack propagation paths, which can attributed to the synergy of interaction of nano-silica particles with somewhat plasticised epoxy matrix. However, the fracture surfaces of both pure and modified specimens tested at 70 °C show more extensive plastic deformation, as shown in Fig. 9, and the brittle fracture is overwhelmed by the large plastic flow processes at the crack tip. With the increases in temperature the cured pure epoxy become plasticised, with clear reductions in Young's modulus (from 2.8 GPa at RT to 2.56 GPa at 50 °C and 2.37 GPa at 70 °C) and tensile strength (from 74.9 MPa at RT to 56.2 MPa at 50 °C and 44.9 MPa at 70 °C). The increased ductility can lead to a large yielding zone around the crack tip, causing crack-tip blunting before fracture. Hence, the existence of nano-silica particles does not promote any mechanism in increasing the fracture energy in a plasticised matrix at 70 °C. However the crack growth path in the pure epoxy is quite different from that in the epoxies modified with nano-silica, as shown in Fig. 9. The mechanisms behind such phenomena are not clear at the moment.

Low temperatures

The values of K_{IC} at two low temperatures, 0 °C and –50 °C, in comparison with those at RT are shown in Fig. 10. Tensile and flexure properties of the pure and modified epoxies at 0°C and –50 °C are shown in Table 3. With an increase in content of nano-silica, there are noticeable increases in the fracture toughness K_{IC} up to about 20% and 25%, respectively for the nano-silica modified epoxies with 4 wt% nano-silica measured at 0 °C and –50 °C, while tensile and flexural strengths and moduli of the materials remain unchanged or are slightly higher, being similar to the cases at RT. At low temperatures, pinning of the crack front by nano-particles is responsible for increasing fracture toughness, as plastic yielding of the matrix is difficult to achieve [16]. SEM photographs of fracture surfaces of CT specimens (pure and modified epoxies) tested at –50 °C are shown in Fig. 11. The flat fracture surfaces for the pure specimens indicate brittle cleavage failures, but for the nano-silica modified epoxy there are some signs of localized ridgelines behind the crack front line, which can be attributed to crack deflection/twisting through the addition of nano-silica particles. In general appearance, the fracture mechanisms at low temperatures are similar to those at RT, although the influence of nano-silica in increasing fracture toughness is less pronounced than that at RT.

Glass transition temperatures

A summary of T_g measured by DMA is shown in Table 4. At least three specimens were tested for each group and the average values with standard deviations are presented. T_g is around 100–102 °C and it did not show any clear change trend when the content of nano-silica was increased to 8 wt%. Figure 12 shows the typical DMA data measured for the pure epoxy and a 6 wt% nano-silica modified epoxy. Although there were no significant changes in T_g with the addition of

Table 2 Mechanical properties of nano-silica modified epoxies at elevated temperatures

Nano-silica (wt%)	Tensile Modulus [GPa]		Tensile Strength [MPa]		Flexural Modulus [GPa]	Flexural Strength [MPa]
	50 °C	70 °C	50 °C	70 °C	50 °C	50 °C
0	2.56 ± 0.09	2.37 ± 0.16	56.2 ± 0.4	44.9 ± 2.3	2.58 ± 0.15	84.9 ± 1.6
2	2.41 ± 0.13	2.31 ± 0.21	56.5 ± 0.9	42.9 ± 3.4	2.61 ± 0.11	89.0 ± 2.5
4	2.44 ± 0.05	2.34 ± 0.08	56.8 ± 1.0	43.9 ± 1.3	2.70 ± 0.09	85.0 ± 0.9
6	2.58 ± 0.21	2.35 ± 0.12	56.9 ± 0.8	43.1 ± 1.9	2.71 ± 0.07	86.3 ± 1.6
8	2.61 ± 0.18	2.38 ± 0.25	51.3 ± 2.5	42.9 ± 2.9	2.79 ± 0.05	87.4 ± 0.8

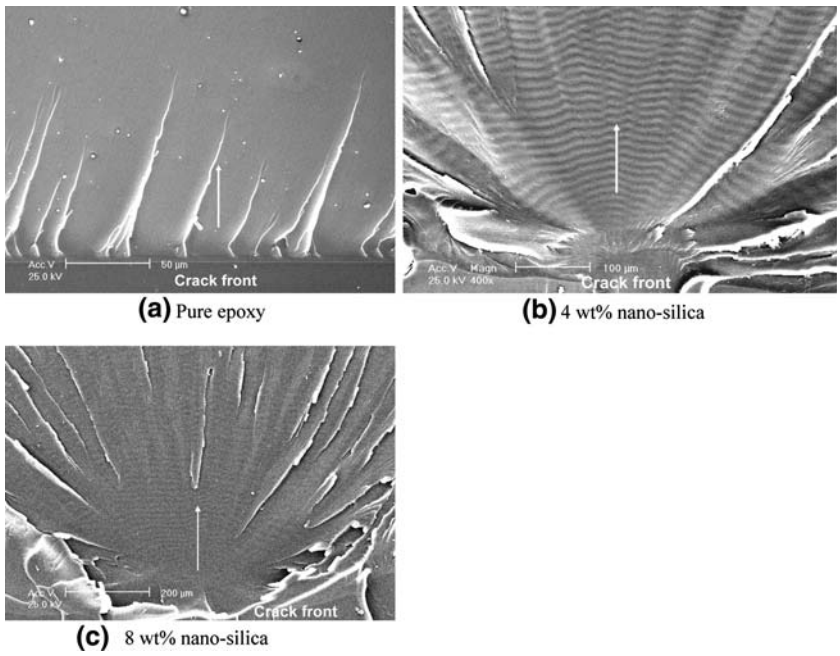

Fig. 8 SEM micrographs of fracture surfaces near crack tips at 50 °C, (**a**) pure epoxy, (**b**) 4 wt% nano-silica, and (**c**) 8 wt% nano-silica

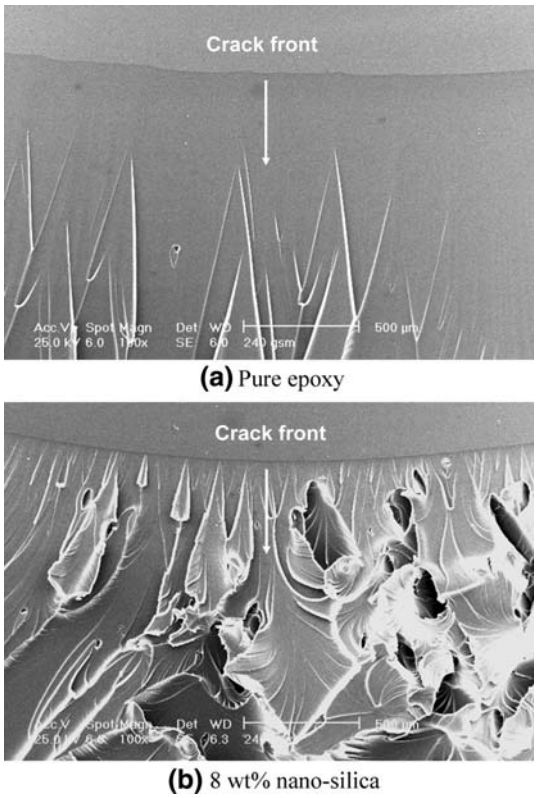

Fig. 9 SEM micrographs of fracture surfaces near crack tips at 70 °C, (**a**) pure epoxy, and (**b**) 8 wt% nano-silica

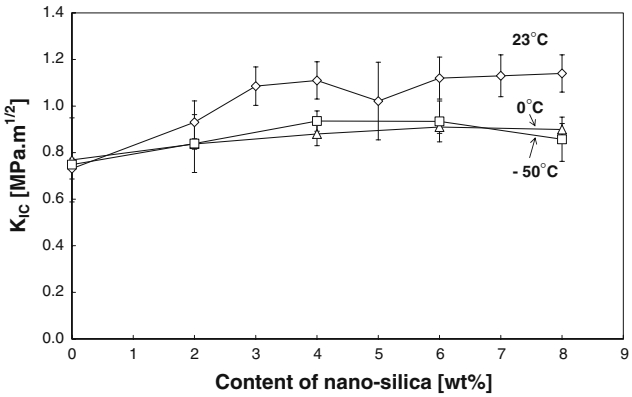

Fig. 10 Fracture toughness of pure/modified epoxies measured at RT, 0 °C and –50 °C

nano-silica, the modified epoxy exhibited higher storage modulus and T_g than the pure epoxy, as shown in Table 4 and Fig. 12.

Conclusions

From the experimental results obtained in this study at low and elevated temperatures from –50 °C to 70 °C, it can be concluded that the nano-silica particles can provide an effective way of increasing the fracture toughness of epoxy resins without sacrificing other properties such as strength, modulus and glass transition temperature. The fracture toughness of the nano-silica modified epoxies was noticeably increased, especially at RT and 50 °C, with the greatest improvement in the systems of around 4–5 wt% nano-silica. However, nano-silica particles do not promote any mechanism to increase fracture energy in a plasticised matrix at 70 °C. At low temperatures the fracture

Table 3 Mechanical properties of nano-silica modified epoxies at low temperatures

Nano-silica (wt%)	Tensile Modulus [GPa]		Tensile Strength [MPa]		Flexural Modulus [GPa]		Flexural Strength [MPa]	
	0 °C	–50 °C	0 °C	–50 °C	0 °C	–50 °C	0 °C	–50 °C
0	2.79 ± 0.07	3.20 ± 0.21	77 ± 4	83 ± 10	3.05 ± 0.15	3.27 ± 0.1w	137 ± 3	189 ± 7
2	2.84 ± 0.08	3.41 ± 0.14	80 ± 5	88 ± 6	2.84 ± 0.14	3.15 ± 0.17	135 ± 7	180 ± 27
4	2.95 ± 0.06	3.46 ± 0.14	81 ± 3	103 ± 9	3.11 ± 0.09	3.30 ± 0.18	141 ± 3	179 ± 8
6	3.04 ± 0.09	3.45 ± 0.13	80 ± 4	90 ± 17	3.04 ± 0.13	3.17 ± 0.07	143 ± 3	190 ± 3
8	3.06 ± 0.13	3.47 ± 0.24	81 ± 5	92 ± 12	3.19 ± 0.09	3.27 ± 0.25	143 ± 3	181 ± 7

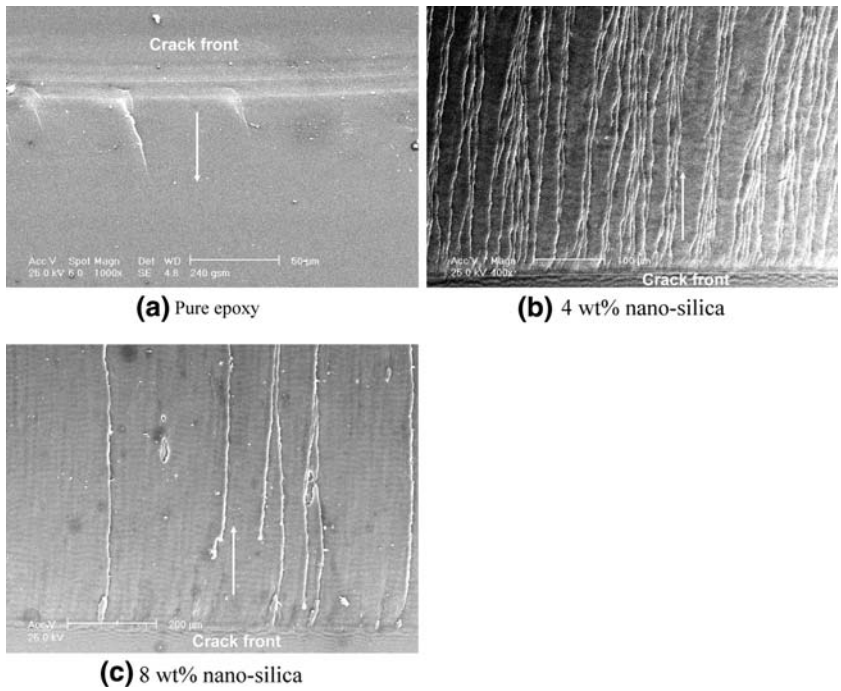

Fig. 11 SEM micrographs of fracture surfaces near crack tips at –50 °C, (**a**) pure epoxy, (**b**) 4 wt% nano-silica, and (**c**) 8 wt% nano-silica

Table 4 Glass transition temperatures of nano-silica modified epoxies

Nano-silica (wt%)	T_g (derived from tan δ)		T_g (derived from E″)	
	Average	SD	Average	SD
0	100.4	0.3	93.5	0.4
2	101.8	0.2	95.3	0.3
4	100.2	0.4	93.4	0.3
6	102.1	0.6	95.6	0.5
8	102.1	0.5	95.3	0.5

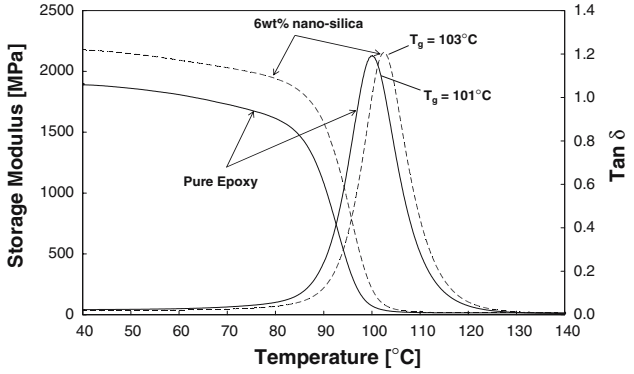

Fig. 12 DMA data for pure and 6% nano-silica modified epoxies

mechanisms are similar to those at RT, although the influence of nano-silica in increasing fracture toughness is less pronounced than that at RT.

It appears that nano-silica particles play different roles when the temperature is changed significantly from low to high, and the mechanisms behind such phenomena certainly need further elaboration.

Acknowledgement The authors thank C. Liu and H. Yang for their help in specimen preparation and conducting experiments. L Ye thanks the Alexander von Humboldt Foundation for the Friedrich Wilhelm Bessel Award for his research stay in Germany in 2005.

References

1. Garg AC, Mai YW (1988) Compos Sci Technol 31:179
2. Bascom WD, Cottington RL, Jones RL, Peyser P (1975) J Appl Polym Sci 19:2545
3. Hodgkin JH, Simon GP, Varley RJ (1998) Polym Adv Technol 9:3
4. Kinloch AJ, Taylor AC (2003) J Mater Sci Lett 22:1439
5. Moloney AC, Kausch HH, Stieger HR (1983) J Mater Sci 18:208
6. Kinloch AJ, Lee JH, Taylor AC, Sprenger S, Eger C, Egan D (2003) J Adhesion 79:867
7. Liu Y-L, Lin Y-L, Chen CP, Jeng RJ (2003) J. Appl. Polym. Sci. 90:4047
8. Kinloch AJ, Mohammed RD, Taylor AC, Eger C, Sprenger S, Egan D (2005) J Mater Sci 40:5083
9. Huang CJ, Fu SY, Zhang YH, Lauke B, Li LF, Ye L (2005) Cryogenics 45:450
10. Xiao K, Ye L, Kwok YS (1998) J Mater Sci 33:2831
11. Abdelkader AF, White JR (2005) J Mater Sci 40:1843
12. Bicerano J, Seits JT (1996) In: Arends CB (ed) Polymer toughneing, Marcel Dekker, Inc, New York, p. 41
13. Faber KT, Evans AG (1983) Acta Metall 31:565
14. Garg AC, Mai YW (1988) Compos Sci Technol 31:225
15. Kinloch AJ, Maxwell D, Young RJ (1985) J Mater Sci 20:4169
16. Kinloch AJ, Maxwell D, Young RJ (1985) J Mater Sci Lett 4:1276